Electronic Supplementary Information

Ms. ID: LC-ART-06-2015-000731

17 July, 2015

Paper Diagnostic Device for Quantitative Electrochemical Detection of Ricin at Picomolar Levels

Josephine C. Cunningham,[a] Karen Scida,[a] Molly R. Kogan,[a] Bo Wang,[b] Andrew D. Ellington,[b] and Richard M. Crooks[a,*]

[a]Department of Chemistry, The University of Texas at Austin, 105 E. 24th St., Stop A5300, Austin, TX, 78712 USA

[b]Department of Microbiology, The University of Texas at Austin, 2500 Speedway, MBB 3.424, Austin, TX, 78712 USA

17 Pages

Table of Contents

Conventional electrochemical cell. Some electrochemical experiments were carried out using a conventional electrochemical cell (Figure S1). This cell is configured with a glassy carbon working electrode (GCE) inserted into a hole at the bottom of the cell, and the reference (Hg/Hg_2SO_4) and counter (Pt) electrodes are inserted into the top (Figure S1a). The dimensions of the PTFE electrochemical cell are provided in Figure S1b.

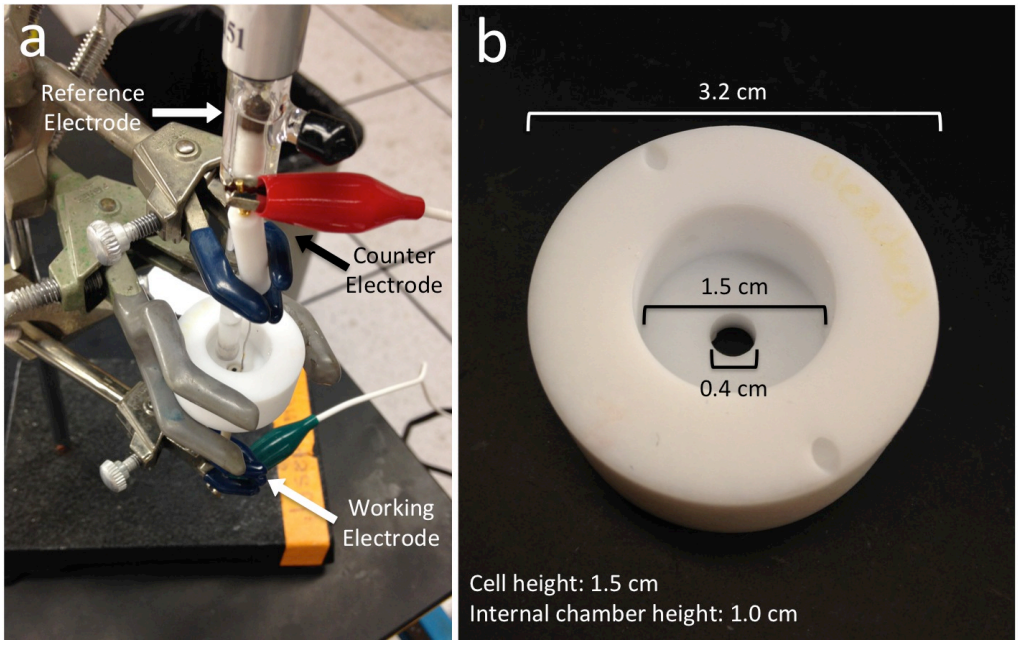

Figure S1. (a) A photograph of the conventional electrochemical. (b) Dimensions of the polytetrafluoroethylene (PTFE) cell in (a).

***o*Slip fabrication.** The oSlip was fabricated as follows. First, a sheet of chromatography paper is wax patterned (using the wax printer) with multiple *o*Slips, each one containing the design shown in Scheme 1 (main text). Second, the wax is melted through the thickness of the paper to create hydrophobic barriers by placing it in an oven at 130 °C for 30 s. The hemi-channel on Layer 4 of the *o*Slip (Scheme 1) is made using 60% yellow wax (specified in Adobe Illustrator CS6) that does

not melt through the entire thickness of the paper, and therefore creates a hydrophilic floor to drive capillary flow in the *o*Slip hollow channel.[1] Third, the individual devices are cut around the exterior edge with scissors or a laser engraving system (laser cutter). At this point the inlet on Layer 1 and void spaces on Layer 2 and 3 are also removed with a razor blade or laser cutter.

Following the first three basic fabrication steps, the electrodes are stencil printed onto Layer 1, such that upon folding they are in contact with the open channel of Layer 2. The electrode design was created using Adobe Illustrator CS6 and cut into a stencil using the laser cutter. The resulting stencil was aligned with the paper, and then thickened carbon paste was scraped across the surface of the stencil until all void spaces were filled with ink. The carbon ink was thickened by placing a ~0.5 cm-thick layer of the commercial paste into a glass petri dish and removing some solvent by heating in an oven at 65 °C for three 30 min intervals. Between each heating interval the paste layer was mixed with a glass rod. The thickened paste was stored at 4 – 8 °C until used. Finally, copper tape was attached directly onto the electrode leads to serve as contacts, and blue dye was dried (under ambient air) on Layer 2 of the *o*Slip.

Unoptimized immunocomposite formation protocol. Before optimization, the formation of the full ricin *a* chain immunocomposite was performed by first placing 15.0 μL of the magnetic microbead/43RCA anti-ricin *a* chain antibody conjugate in a microcentrifuge tube, removing the supernatant by magnetic separation, and simultaneously adding 25.0 µL of the AgNP/AB-RIC-mAb2 anti-ricin *a* chain antibody conjugate and

25.0 μL of various concentrations of ricin *a* chain (diluted in 0.10 M borate solution (pH 7.5)). Second, the resulting mixture was incubated for 1 h while mixing. Third, the full sandwich immunocomposite (magnetic microbead/anti-ricin *a* chain 43RCA antibody/ricin *a* chain/anti-ricin *a* chain AB-RIC-mAB2 antibody/AgNP) was washed twice with 50.0 μL of 0.10 M borate solution (pH 7.5). Note that all of the mixing steps were performed at 1500 rpm and 24 °C on the BioShake iQ thermomixer, and all washing steps were done by magnetic separation.

ELISA detection protocol. An enzyme linked immunosorbent sandwich assay (ELISA) detection method was used to rapidly optimize the variables associated with formation of the immunocomposite. Note that all of the mixing steps were performed at 1500 rpm and 24 °C using the BioShake iQ thermomixer, and all washing steps were carried out by magnetic separation. This was achieved by removing the supernatant of the immunocomposite, resuspending in 20.0 μL of the anti-mouse HRP-containing antibody (in a 1:2500 dilution in 0.10 M borate solution at pH 7.5), and incubating for 1 h while mixing. Next, the resulting conjugates were washed twice with 20.0 μL of 0.10 M borate solution (pH 7.5) and reacted with 50.0 μL of stock TMB solution. After 2.00 min, the reaction between the TMB substrate and HRP was quenched by adding 50.0 μL of 1.0 M H_2SO_4. Using a magnet, 50 μL of the colored supernatant was transferred to a microplate well. Finally, the resulting absorbance was measured at 450 nm using a microtiter plate reader.

AgNP oxidation by bleach (ClO^-). Confirmation of the spontaneous oxidation of AgNPs by ClO^- was obtained by TEM. In this experiment, two individual aliquots of AgNPs were dried in air for 12 h on different TEM grids. The first aliquot contained 125.0 pM AgNPs in water and the second contained 125.0 pM AgNPs in an aqueous solution of 30.9 mM ClO^-. Figure S2a shows two modes in the particle size distribution for the first aliquot: one at 5 ± 2 nm (believed to be the AgNP seeds from which Ag growth was initiated during synthesis), and the other at 19 ± 4 nm. However, no AgNPs were observed in the second aliquot (even at high magnification), thereby confirming complete oxidation of the AgNPs by ClO^-. Figure S2b is a TEM of the first sample with no ClO^- present, where the particles are clearly observed to have size of ~20 nm.

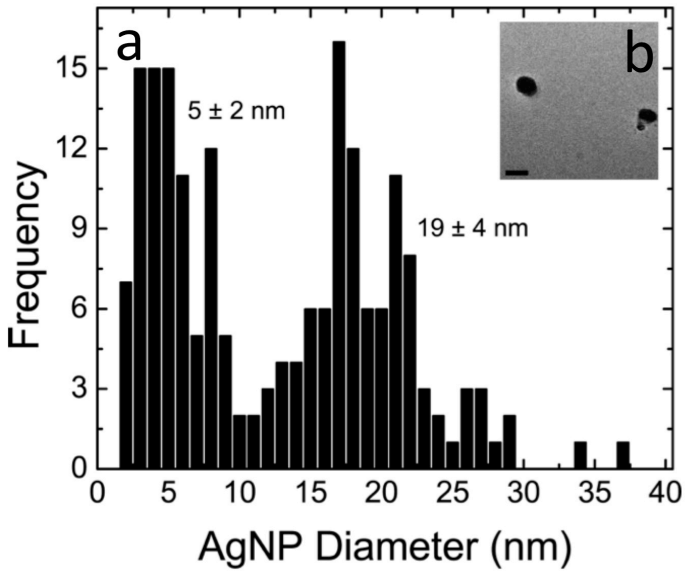

Figure S2. (a) Size-distribution histogram for AgNPs in the absence of ClO^-. (b) An image of the AgNPs in the absence of ClO^-. The black bar at bottom-left corner of the inset represents 20 nm.

Optimization of ricin immunocomposite formation. Optimization of the formation of the immunocomposite was performed in six steps starting with the unoptimized immunocomposite formation protocol and using ELISA as the detection method (for rapid screening). Importantly, each consecutive optimization step was performed starting with the optimum condition(s) determined in the previous step(s). Optimization was carried out using 4 μg/mL of ricin *a* chain.

First, the concentration of the MμB/anti-ricin *a* chain 43RCA antibody conjugate was varied while keeping the concentrations of ricin *a* chain and AgNP/anti-ricin *a* chain AB-RIC-mAb2 antibody conjugate constant (4 μg/mL and 2.3 x 10^{11} AgNPs/mL, respectively). Figure S3a shows that the signal increases with higher amounts of

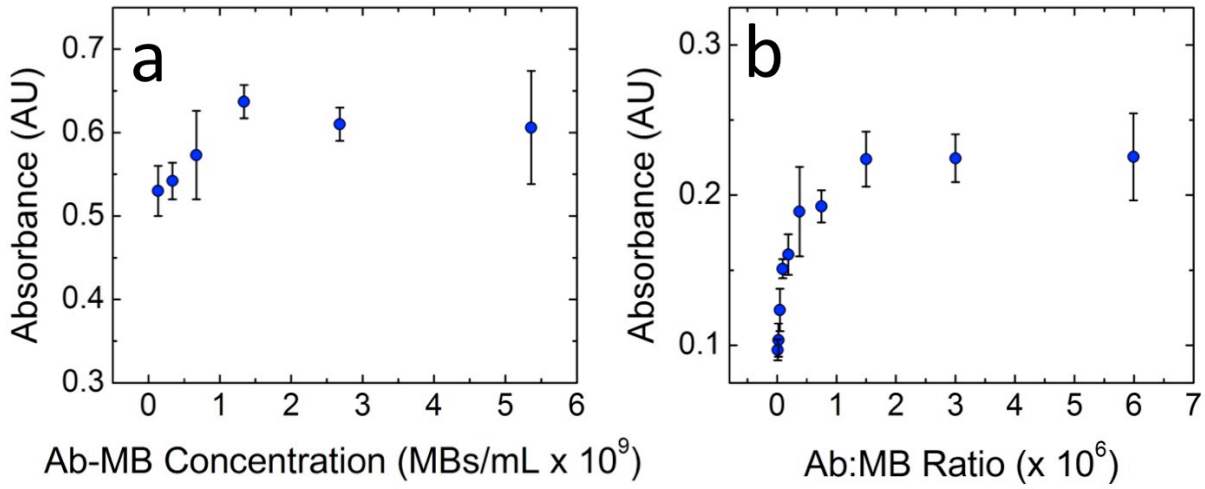

Figure S3. Optimization of the magnetic microbead antibody conjugate conditions for the ricin *a* chain immunocomposite formation using the ELISA detection strategy. Optimized variables: (a) magnetic microbead antibody conjugate concentration and (b) antibody to magnetic microbead ratio.

MμB/anti-ricin *a* chain 43RCA antibody conjugate added (MμB/Ab, concentration expressed as MμBs/mL) up to about 1.3 x 10^9 MμBs/mL.

At higher concentrations the signal plateaus. From this plot, the concentration of MμB/anti-ricin *a* chain 43RCA antibody conjugate selected for further optimization steps was $1.5x10^9$ MμBs/mL.

In the second optimization step the ratio of anti-ricin *a* chain 43RCA antibody to MμB was optimized by varying the concentration of antibody used in the antibody to MμB conjugation procedure. Figure S3b shows that the absorbance increases with increasing antibody concentration and plateaus at approximately 1.5×10^6 Ab:1 MμB. To ensure that an excess of antibody is present during conjugation, 3.0×10^6 Ab:1 MμB was used for all subsequent experiments.

The third and fourth optimization steps involved varying the borate solution concentration and pH. In both cases, the conditions used to form the AgNP/anti-ricin *a* chain AB-RIC-mAb2 antibody conjugate were varied based on a previously reported optimization approach for conjugating antibodies to AgNP conjugation.[2] The borate concentration was optimized by varying its concentration while keeping all other conditions constant. Figure S4a shows that the absorbance increased with decreasing borate solution concentration with a maximum at 1.0 mM borate. On the basis of the histogram, a borate concentration of 1.0 mM was selected for further optimization. The borate solution pH was optimized by varying the pH of the 1.0 mM borate solution used for the antibody to AgNP conjugation. Figure S4b shows that the absorbance signal increases with increasing pH to a maximum at pH 9. On the basis of these results, pH 9 was selected for use in future experiments.

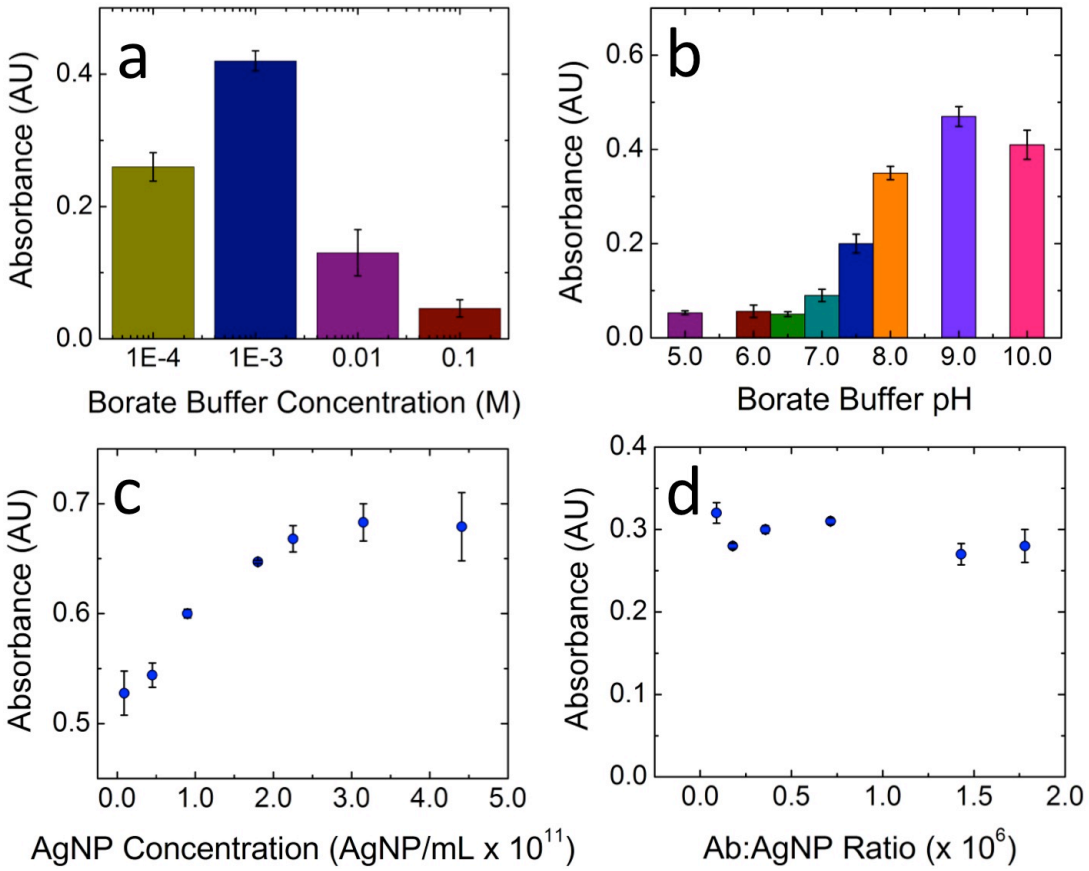

Figure S4. Optimization of the AgNP/antibody conjugation conditions for the ricin *a* chain immunocomposite formation using the ELISA detection strategy. Optimized variables: (a) borate solution concentration during the AgNP conjugation protocol; (b) pH of the borate solution used for AgNP conjugation; (c) AgNP antibody conjugate concentration; and (d) antibody-to-AgNP ratio.

The fifth step focused on optimizing the concentration of the AgNP/anti-ricin *a* chain AB-RIC-mAb2 antibody conjugate while keeping the concentrations of ricin *a* chain and MμB/anti-ricin *a* chain 43RCA antibody conjugate constant (4.0 μg/mL and 1.5 x 10^9 MμBs/mL, respectively). Figure S4c shows that the signal increases with higher amounts of AgNP/anti-ricin *a* chain AB-RIC-mAb2 antibody conjugate added (AgNP/Ab, concentration expressed as AgNPs/mL). At concentrations higher than 2.2 x 10^{11} AgNPs/mL, the signal plateaus.

From this plot, the concentration of AgNP/anti-ricin *a* chain AB-RIC-mAb2 antibody conjugate selected for further optimization steps was 3.0×10^{11} AgNPs/mL.

The sixth optimization step involved varying the anti-ricin *a* chain AB-RIC-mAb2 antibody concentration during the antibody-to-AgNP conjugation procedure. Figure S4d shows that the amount of antibody on the AgNPs is not important as long as there are enough antibodies present to stabilize the AgNPs. Specifically, a minimum of 10 μg/mL of anti-ricin *a* chain AB-RIC-mAb2 antibody is required during conjugation or else the AgNPs aggregate, turning the solution from yellow to colorless. Consequently, all antibody concentrations less than 10 μg/mL are not included in Figure S4d. A ratio of 1×10^5 Ab:1 AgNP was selected for use in all future experiments.

After the last optimization step, a dose-response curve was obtained that resulted in Figure S5. Here, the optimized values for the one-step immunocomposite formation were used and the concentration of ricin *a* chain was varied from 0.010 to 2.71 μg/mL (dilutions were carried out in 0.10 M borate solution, pH 7.5). The LOD (calculated as three times the standard deviation of the blank signal, divided by the slope) was determined to be 0.63 nM.

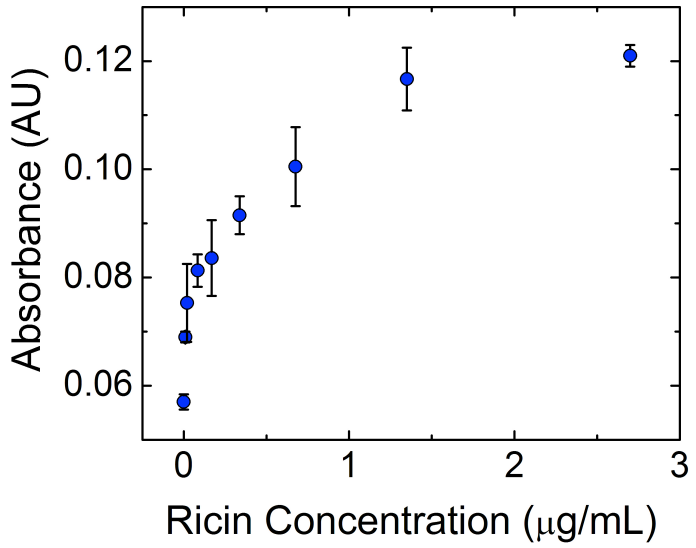

Figure S5. A dose-response curve for ricin *a* chain using the ELISA detection method after optimizing all immunocomposite formation conditions.

Stability of hypochlorite in water. Although ClO^- is known for being unstable as a salt, its decomposition in water is relatively slow at neutral and alkaline pH.[3] Therefore, stock aqueous solutions of ClO^- can be used for long periods of time without losing equivalents of oxidant due to long-term storage.

Effect of hypochlorite on the working electrode surface. It is important to know if the oxidant, or any of its oxidized/reduced forms, has any negative effects on the surface of the working electrode (WE). Specifically, if the WE surface is affected (e.g., oxidized), then the desired electrochemical signal and sensitivity of the assay will also be affected. The following experiment was designed to study the stability of the electroactive surface area of the WE under the conditions required for operation of the *o*Slip experiments.

The following experiments were carried out in a conventional electrochemical cell. First, a cyclic voltammogram (CV) was obtained using a solution containing 125.0 μL BCl (0.10 M boric acid plus 0.10 M NaCl, pH 7.5), 100.0 μL of water, and 1.03 mM 1,1′-ferrocenedimethanol (FDM). Second, the GCE was removed from the solution, rinsed with DI water, and placed in a solution of 125.0 μL BCl, 100.0 μL water, and 0.31 M ClO^-. At this point, the potential of the glassy carbon electrode (GCE) was held at E = -0.9 V for t = 200 s to simulate the electrodeposition conditions used in *o*Slip experiments. Third, the GCE was rinsed with DI water, placed back in 125.0 μL of the BCl solution containing 1.03 mM FDM, and a second CV was obtained. As shown in Figure S6, the FDM electrochemical response did not change after exposing the GCE to high concentrations of ClO^- during the electrodeposition step. These results provide evidence for the stability of the WE surface under the experimental conditions required for Ag detection in the *o*Slip.

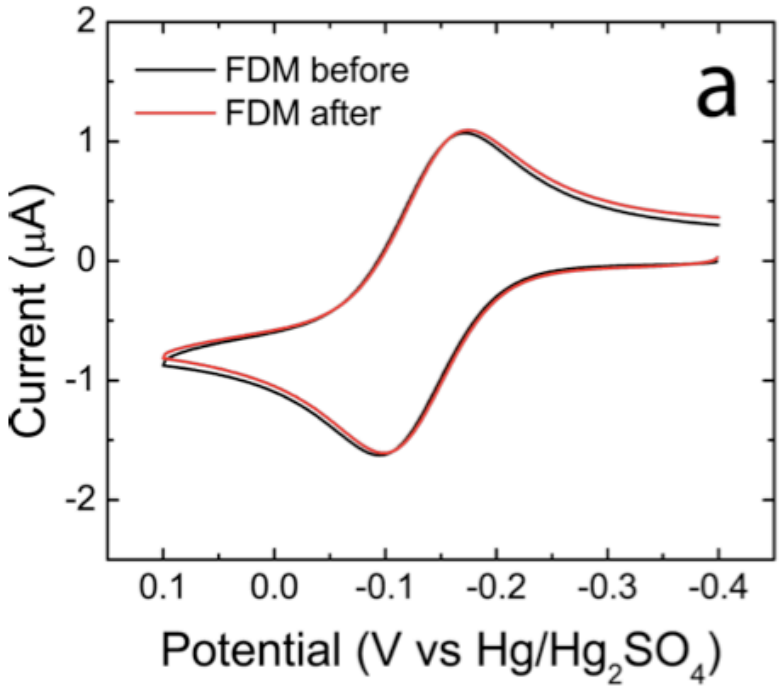

Figure S6. Cyclic voltammogram of FDM before (black trace) and after (red trace) applying E = - 0.60 V for t = 200 s in the presence of 0.31 M ClO^- (no Ag present). Conditions: WE = GCE (1.0 mm diameter), RE = Hg/Hg_2SO_4 (sat), CE = Pt wire, ν = 100 mV/s.

Although ClO^- is better than MnO_4^-, the oxidant we used in our previous work,[4] in terms of its stability in water and its not reacting to produce an insulating layer on the surface of the WE, it also suffers from some limitations. For example, the two main disadvantages are that the Ag ASV signal (charge) rapidly decreases at high ClO^- concentrations due to high baseline currents arising from ClO^- reduction (Figure 1b and Figure 3a in the main text) and the poor stability of bleach when dried on paper (further explained below).

Stability and re-solvation of dried bleach on the *o*Slip. One important factor to consider in the selection of the ideal oxidizing agent is its long-term stability on the slip layer (Layer 3) of the

*o*Slip. Accordingly, five different experiments were performed to test the stability of ClO^- when dried on paper. In the first experiment, 4.0 μL of an aqueous solution containing 0.13 M ClO^- was added to 125.0 μL BCl and 96.0 μL of DI water, mixed thoroughly, and a CV was obtained using the conventional electrochemical cell. This CV (black trace in Figure S7) served as a point reference indicating 100% of the signal corresponding to the amount of ClO^- used. The peak at ~-0.50 V corresponds to reduction of ClO^- and the peak at ~-1.0 V is attributable to oxygen reduction.

In the second experiment, the same amount of ClO^- was dried by gentle N_2 flow (fast drying) on the paper-based reagent storage tab on Layer 3 of the *o*Slip. When the solution was completely dry (in about 1 min), the paper tab was detached (using a razor blade) and immediately immersed in a solution containing 125.0 μL BCl and 100.0 μL DI water. The solution was mixed thoroughly for 30 s, and then the red CV in Figure S7 was obtained. Here, a decrease in the peak current corresponding to ClO^- reduction is observed, which could be due to either partial decomposition of ClO^- during the drying process or incomplete rehydration of ClO^- from the paper zone. Nevertheless, the majority of the ClO^- dried using gentle N_2 flow is still available in the oxidized form for the *o*Slip experiments.

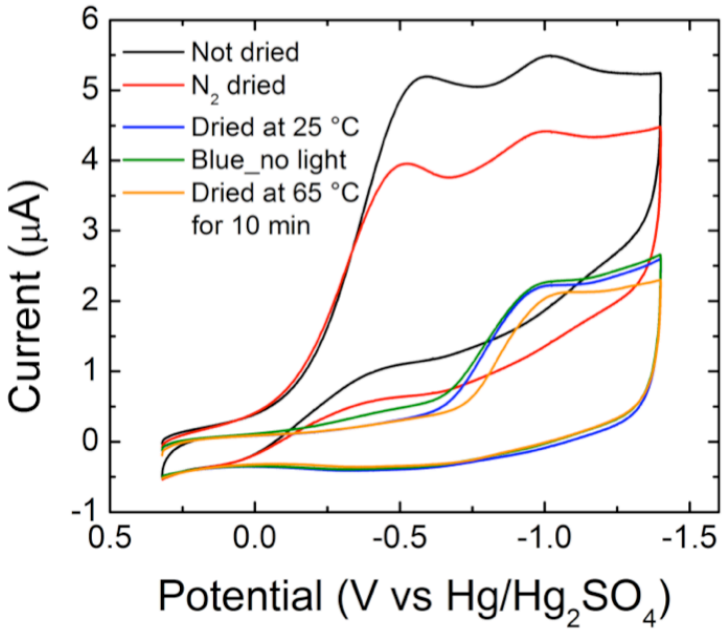

Figure S7. CVs illustrating the relative ability to dry ClO^- (4 μL, 0.13 M) and rehydrate (with 125.0 μL BCl and 96.0 μL of DI water) on the paper-based reagent delivery tab. Conditions: WE = GCE (1.0 mm diameter), RE = Hg/Hg_2SO_4 (sat), CE = Pt wire, ν = 100 mV/s.

The third experiment was performed in a similar manner to the second experiment, with one exception: ClO^- was dried at 25°C in open air for 1 h. In this case, ClO^- completely decomposed during the drying process as no current is observed for the reduction of ClO^- at E = -0.5 V (Figure S7, blue trace). Likewise, when ClO^- was dried in the absence of light or in an oven at 65 °C (for faster drying) no current corresponding to the reduction of ClO^- is observed (Figure S7, green and orange traces, respectively). We conclude that ClO^- is not stable in air after evaporation of water, and therefore ClO^- cannot be stored for long periods of time on paper without air-free packaging.

After Layer 3 is slipped to bring the paper tab with pre-dried ClO^- into direct proximity of the AgNP labels and WE, a certain amount

of time needs to elapse before the resulting Ag^+ is collected. This is the time required for rehydration and diffusion of ClO^- from the paper tab to the AgNPs. To determine the optimal wait time, the optimized ricin immunocomposite (formed with 4 µg/mL ricin *a* chain) was injected into the *o*Slip. Then, after slipping Layer 3 of the *o*Slip, with 2.0 µL of 13.5 mM ClO^- pre-dried on the paper tab, various amounts of time were allotted before initiating ASV detection. Figure S8 shows that no Ag ASV charge is detected using a wait time of 10 s and that the largest charge is observed after waiting 12 s. The rapid decrease in Ag signal after 12 s is attributed to the diffusion of Ag^+ away from the WE.

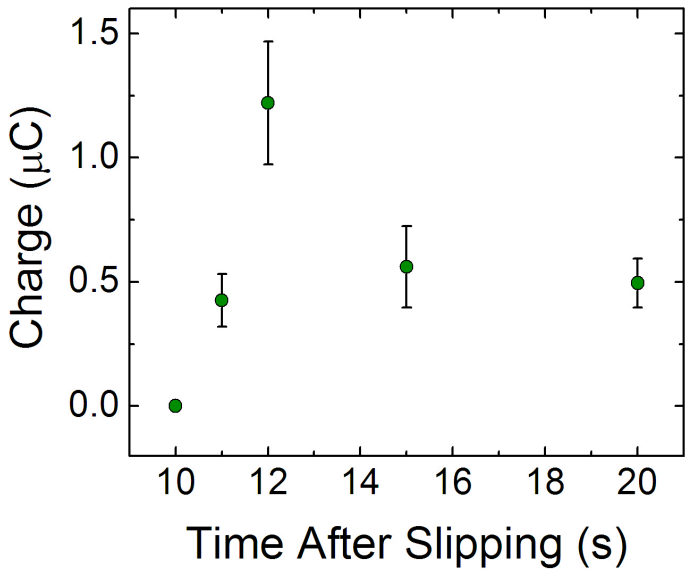

Figure S8. Determination of the optimal wait time (12 s) between slipping in the ClO^- oxidant and starting Ag electrodeposition.

References

(1) C. Renault, X. Li, S. E. Fosdick and R. M. Crooks, *Anal. Chem.*, 2013, **85**, 7976–7979.

(2) M. S. Szymanski and R. A. Porter, *J. Immunol. Methods*, 2013, **387**, 262–269.

(3) Pourbaix, M., National Association of Corrosion Engineers, 1974.

(4) K. Scida, J. C. Cunningham, C. Renault, I. Richards and R. M. Crooks, *Anal. Chem.*, 2014, **86**, 6501–6507.